FUSE observations of the *HI* interstellar gas of I Zw 18

A. A. Lecavelier Des Etangs, J.-M. Désert, D. Kunth, A. Vidal-Madjar, G. Callejo, R. Ferlet, G. Hébrard, Vianney Lebouteiller

A&A 413, 131–137 (2004)
DOI: 10.1051/0004-6361:20031518

Astronomy & Astrophysics

FUSE observations of the H I interstellar gas of I Zw 18

A. Lecavelier des Etangs[1], J.-M. Désert[1], D. Kunth[1], A. Vidal-Madjar[1], G. Callejo[1,2], R. Ferlet[1], G. Hébrard[1], and V. Lebouteiller[1]

[1] Institut d'Astrophysique de Paris, CNRS, 98 bis Bld Arago, 75014 Paris, France
[2] LERMA, Observatoire de Paris – Section de Meudon, 5 place Jules Janssen, 92195 Meudon Cedex, France

Received 28 May 2003 / Accepted 20 September 2003

Abstract. We present the analysis of *FUSE* observations of the metal-deficient dwarf galaxy I Zw 18. We measured column densities of H I, N I, O I, Ar I, Si II, and Fe II. The O I/H I ratio ($\log(\mathrm{O\,I/H\,I}) = -4.7^{+0.8}_{-0.6}$) is consistent with the O/H ratio observed in the H II regions (all uncertainties are 2-σ). If the oxygen is depleted in the H I region compared to the H II regions, the depletion is at most 0.5 dex. This is also consistent with the log(O/H) ratios ∼−5 measured with *FUSE* in the H I regions of other blue compact dwarf galaxies. With $\log(\mathrm{N\,I/O\,I}) = -2.4^{+0.6}_{-0.8}$, the measured N I/O I ratio is lower than expected for primary nitrogen. The determination of the N II column density is needed to discriminate between a large ionization of N I or a possible nitrogen deficiency. The neutral argon is also apparently underabundant, indicating that ionization into Ar II is likely important. The column densities of the other α-chain elements Si II and Ar I favor the lower edge of the permitted range of O I column density, $\log(N_{\mathrm{cm}^{-2}}(\mathrm{O\,I})) \sim 16.3$.

Key words. line: profiles – galaxies: abundances – galaxies: dwarf – galaxies: ISM – galaxies: individual: I Zw 18 – ultraviolet: galaxies

1. Introduction

I Zw 18 (Mrk 116) is a blue compact dwarf galaxy with the smallest known abundance of heavy elements as measured from nebular emission lines. The observed emission lines originate from a pair of bright H II regions in which a strong burst of star formation is taking place. In these H II regions, the oxygen abundance is measured to be only ∼1/50 the solar value (Izotov et al. 1999). The interstellar gas ionized by recently formed massive stars is surrounded by an envelope of neutral hydrogen (H I). This envelope has been extensively observed through 21cm radio maps which give a total mass of $M_{\mathrm{HI}} \sim 5\times10^7\ M_\odot$ (Lequeux & Viallefond 1980; Viallefond et al. 1987; van Zee et al. 1998).

The composition of this H I gas has been debated. For instance, it had been suggested that it may be a significant reservoir of molecular hydrogen representing a significant fraction of the dark matter (Lequeux & Viallefond 1980). In fact, early *FUSE* (Far Ultraviolet Spectroscopic Explorer; Moos et al. 2000) observations proved that diffuse molecular hydrogen is very scarce with a column density ratio $N_{\mathrm{H_2}}/N_{\mathrm{HI}} < 10^{-6}$ (Vidal-Madjar et al. 2000).

Also there is a disagreement about the metallicity of the neutral gas. Kunth & Sargent (1986) postulated the importance of the "self-pollution" of heavy elements in the H II regions by the present star burst. They suggested that the neutral gas might be more primordial than the H II regions and close to zero metallicity, providing thus a new interesting site to determine the primordial abundances of key elements like deuterium and helium (Kunth et al. 1995). HST has been used to test this hypothesis through the observation of the O I line at 1302 Å. O I is indeed one of the major tracer of the metallicity. The ionization potential of O I is very close to that of H I and the charge exchange between O II and H I is very efficient. Hence the coupling of the oxygen and hydrogen ionization fractions is very strong. In the neutral gas, the O I/H I ratio can therefore be considered as a very good proxy for the O/H ratio and hence for the metallicity.

Unfortunately the O I line at 1302 Å has a very strong oscillator strength ($f_{1302} = 51.9\times10^{-3}$). With an intrinsic line width of $b \sim 18$ km s^{-1} in the case of I Zw 18, and for the metallicity of the ionized gas $Z_{\mathrm{HII\ IZw18}} \sim 1/50\ Z_\odot$, this O I line is strongly saturated already at $N_{\mathrm{HI}} \gtrsim 2\times10^{20}$ cm^{-2}, while the observed N_{HI} is $\geq 2\times10^{21}$ cm^{-2}. As a result, despite deep HST observations, the oxygen abundance is still an open question (Kunth et al. 1994; Pettini et al. 1995). Using also the O I line at 1302 Å, Thuan et al. (1997) claimed that the H I envelope of the dwarf galaxy SBS 0335-052 was extremely metal deficient with an O I/H I ratio $\lesssim 3\times10^{-7}$. However in that same galaxy the O I/H I ratio was subsequently found to be much higher using *FUSE* observations of O I lines at shorter wavelengths and with smaller oscillator strengths (Lecavelier des Etangs et al. 2002;

Send offprint requests to: A. Lecavelier des Etangs,
e-mail: lecaveli@iap.fr

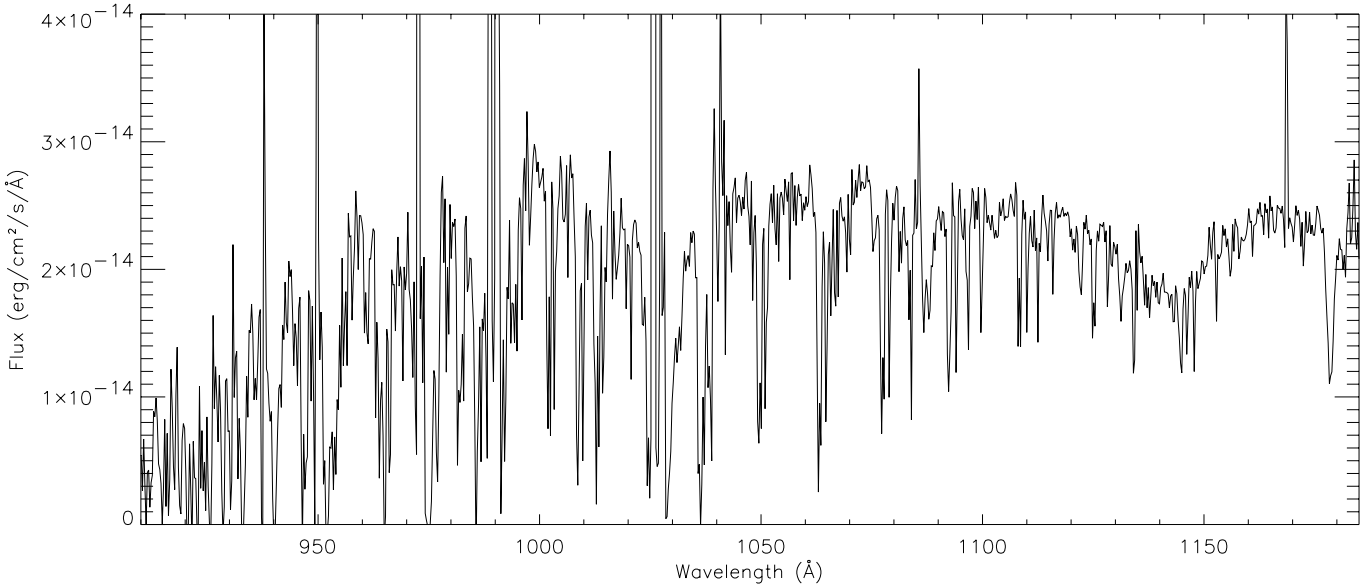

Fig. 1. Plot of the full *FUSE* spectrum of I Zw 18. It is obtained through the addition of all the channels, rebinned by 0.3 Å. In addition to the Earth airglow emission lines and an artifact dip around 1145 Å, many absorption lines from the Milky Way and I Zw 18 are clearly visible. For instance, even at this low resolution, we can see the H I Lyman β, γ, δ, and ϵ lines from I Zw 18 at 1030, 975, 952, and 940 Å, respectively.

Thuan et al. 2003). In fact, the hypothesis of an O I line at 1302 Å unsaturated was simply erroneous.

It is clear that the far-UV is unique for offering a large collection of lines of different elements with a wide range of oscillator strengths. We therefore observed I Zw 18 with *FUSE* to determine the abundances of various species, and constrain the metallicity and the history of elements in one of the most extreme blue compact dwarf galaxy.

In Sect. 2 we describe the observations. In Sect. 3 we present the analysis of the absorption lines against the stellar continuum from the blue massive stellar clusters. Results are presented in Sect. 4 and discussed in Sect. 5. A comparison with *FUSE* observations of other metal-deficient dwarf galaxies will be part of a forthcoming paper (Lebouteiller et al. 2003).

2. Observation

I Zw 18 was observed with *FUSE* (900–1200 Å, see Moos et al. 2000) and Sahnow et al. 2000) through the LWRS aperture (30″ × 30″) for a total of 31 650 s on November 27, 1999 (Program P1980102) and 63 450 s on February 11, 2002 (Program P1080901). During the early observations of November, 1999 (Vidal-Madjar et al. 2000), the *SiC* channels acquisition failed and the resulting spectrum was limited to wavelengths longward of about 1000 Å. Therefore, the *SiC* wavelength range (~900–1000 Å) was only exposed for 63 450 s. The data have been reprocessed with the version 2.0.1 of the `CALFUSE` pipeline. The output of the pipeline is a total of 38 sub-exposures which have been aligned and co-added, resulting in a set of four independent spectra, one for each *FUSE* channel (two *LiF* spectra and two *SiC* spectra).

Many absorption lines are clearly detected (Fig. 1). For a given element, they consist of three main absorbing components at heliocentric radial velocities: -160 km s^{-1}, $\sim$0 km s^{-1}, and 750 km s^{-1} (Vidal-Madjar et al. 2000). These can easily be identified respectively with a known Galactic high velocity cloud at -160 km s^{-1}, the interstellar medium of the Milky Way at low radial velocity, and I Zw 18 itself at 750 km s^{-1} corresponding to a Doppler shift of about $\Delta\lambda \sim 2.5$ Å at 1000 Å. The high velocity cloud is detected in H I, C II, N I, O I, Fe II, and Fe III lines. The Galactic clouds appear in C I, C I*, C II, C III, N I, O I, Si II, Ar I, Fe II, Fe III, and also in molecular hydrogen (H_2). H_2 lines are detected up to the $J = 5$ level. These electronic transitions of H_2 only show up in the Galactic medium. Finally I Zw 18 absorption is detected in H I, C II, C III, N I, O I, S III, Ar I, Si II, Fe II, and Fe III.

In addition to these three main components, O VI lines are detected around 1032 Å and 1037 Å. They correspond to coronal gas with radial velocities between -125 km s^{-1} and +110 km s^{-1}, originating in the Galactic halo (Savage et al. 2003; Sembach et al. 2003; Wakker et al. 2003). As already shown by Vidal-Madjar et al. (2000), no line from H_2 is observed at the radial velocity of I Zw 18. This absence of diffuse molecular hydrogen is also observed in the blue compact dwarf Mrk 59 (Thuan et al. 2002) and is well explained by the low abundance of dust grains, the high ultraviolet flux, and the low density of the H I gas.

3. Method

Column densities have been calculated through profile fitting using the `Owens` procedure developed by Martin Lemoine and the *FUSE* French team. This code returns the most likely values of many free parameters like the Doppler widths and column densities through a χ^2 minimization of the difference between the observed and computed profiles. The latest version of this code is particularly suited to the characteristics of *FUSE*

Table 1. Column densities measured in the *FUSE* spectrum of I Zw 18.

Species	$\log_{10}(N_{\mathrm{cm}^{-2}})$	2-σ error bars
H I	21.30	$^{+0.10}_{-0.10}$
N I	14.22	$^{+0.14}_{-0.17}$
O I	16.60	$^{+0.80}_{-0.55}$
Ar I	13.45	$^{+0.20}_{-0.25}$
Si II	14.80	$^{+0.25}_{-0.25}$
Fe II	14.60	$^{+0.12}_{-0.10}$

spectra. For example, it allows for a variation of the background level, for an adjustable line spread function as a function of the wavelength domain, and for shifts in wavelength scale. These are taken as free parameters which depend on the wavelength region and are determined by the χ^2 minimization. Special attention was paid to the background residual which is not negligible for this faint target. It is found to lie between -6 and $+4\times10^{-15}$ erg cm^{-2} s^{-1} Å^{-1}. The line spread function is mainly constrained by the unresolved Galactic H_2 absorption lines. The resolving power is found to be about $R=\Delta\lambda/\lambda\approx 10\,000$, corresponding to the size of the extended object within the spectroscope slit (Vidal-Madjar et al. 2000).

Values of column densities are given in Table 1 (althrough the paper, error bars are 2-σ). The error bars are estimated by the classical method of the $\Delta\chi^2$ increase of the χ^2 of the fit; see Hébrard et al. (2002) for a full discussion of the fitting method and error estimation with the `Owens` code. These error bars include the uncertainties in the continuum, intrinsic line widths (b), and the instrumental line spread function. It has to be noted that the use of different lines with different oscillator strengths of the same species allows us to constrain all these quantities. In particular, fits of saturated lines constrain the line widths; the instrumental line spread function is mainly constrained through the saturated and very narrow lines from H_2 in the Milky Way. The final results are obtained from a simultaneous self-consistent fit to all the data. We obtain $b_{\mathrm{IZw18}}=17.3\pm5.0$ km s^{-1} (2-σ) for the width of the lines at the I Zw 18 systemic velocity $v_{\mathrm{IZw18}}=750$ km s^{-1}. This is consistent with 21 cm observations (van Zee et al. 1998), which also show that most of the observed line width can be attributed to the velocity gradient of the neutral gas in front of the UV-bright stars.

4. Results

4.1. Column densities

4.1.1. H I

The H I column density in I Zw 18 is derived from all the available lines of the Lyman series. We avoided the blue wing of the Lyman β line and the Lyman γ line, both contaminated by the terrestrial airglow. We fitted the H I Lyman series including the blue wing of the Lyman β line, the Lyman δ, ϵ, ζ, and η lines. Note that the resulting H I column density is mainly constrained by the Lyman β line. We find $N(\mathrm{H\,I})\approx(2.0\pm0.5)\times10^{21}$ cm^{-2} (2-σ uncertainties). This value is consistent with $N(\mathrm{H\,I})\approx2.1\times10^{21}$ cm^{-2} found by Vidal-Madjar et al. (2000) from the early *FUSE* observations. It is also comparable to $N(\mathrm{H\,I})\approx3.5\times10^{21}$ cm^{-2} obtained from *HST/GHRS* observations (Kunth et al. 1994) and to the peak column density of 3.0×10^{21} cm^{-2} of the H I 21 cm observations (van Zee et al. 1998). However with the very different size of the *GHRS* aperture and the VLA synthesized beam, these last values could have been more different, as is the case for the higher column density of about 2×10^{22} cm^{-2} found with the smaller aperture of *HST/STIS* (Brown et al. 2002).

By comparison with H I 21 cm maps, the measured H I column density gives a clue to the location of the absorber. H I column densities of the order of 10^{21} cm^{-2} correspond to the central part of I Zw 18. Such high column densities can be found only within the optical extent of the galaxy. The absorber is thus likely located in the very central part of the galaxy, close to the UV-bright stars and their associated H II regions.

4.1.2. C II and N II

The only strong C II line in the *FUSE* wavelength range is the line at $\lambda_0=1036.3$ Å. Unfortunately, at the I Zw 18 redshift this line is partially blended with an O I airglow emission. It is therefore difficult to obtain a meaningful estimate of the C II column density.

At the redshift of I Zw 18, the N II lines from the ground and excited levels around 1084 Å fall in the *FUSE* detector gap. These lines are only detected at the upper edges of the *SiC* detectors, which are inefficient at these wavelengths. N II column densities cannot be estimated using the present *FUSE* observations.

4.1.3. C III, S III, and Fe III

Absorption lines from highly ionized species are also detected at the I Zw 18 redshift: C III ($\lambda_0=977.0$ Å), S III ($\lambda_0=1012.5$ Å), and Fe III ($\lambda_0=1122.5$ Å). The S III line is blended with Galactic H_2, while the Fe III line is bracketed between Fe II lines from I Zw 18 and from the Milky Way. The C III line is clean and at a slightly different redshift of about 720 km s^{-1} at 979.36 Å (Fig. 2). Voigt profiles give the following column densities: $N(\mathrm{C\,III})\approx4\times10^{13}$ cm^{-2}, $N(\mathrm{S\,III})\approx1\times10^{14}$ cm^{-2}, and $N(\mathrm{Fe\,III})\approx3\times10^{14}$ cm^{-2}.

However, we cannot exclude a blend of those lines with stellar lines. In effect, we find a large intrinsic width for the Fe III line: $b_{\mathrm{FeIII}}\gtrsim90$ km s^{-1}. Consequently, the derived column densities must be considered as upper limits to the true values.

4.1.4. O I

O I is a tracer of the metallicity. The present new *FUSE* data provides the unprecedented opportunity to shed light on a possible metallicity difference between the ionized and the neutral

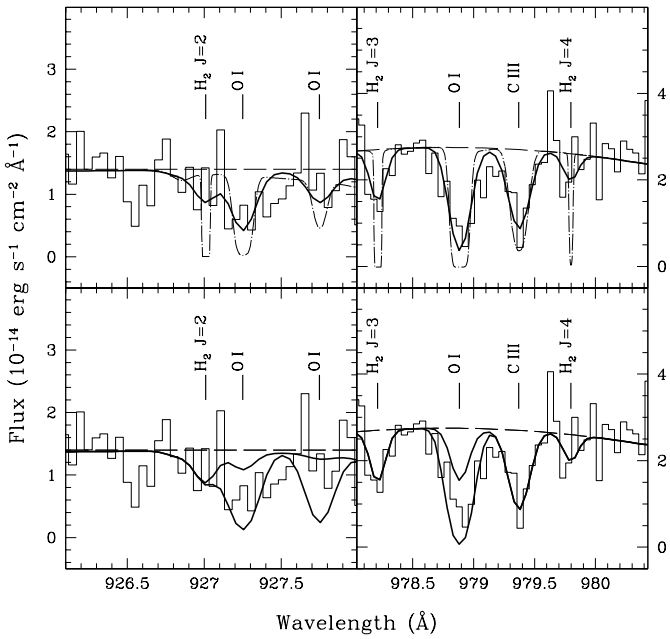

Fig. 2. Sample of O I lines detected at the redshift of I Zw 18 (750 km s^{-1}). The H_2 lines are from the Milky Way. The C III line is at a redshift of 720 km s^{-1}. The histogram shows the data. The upper panels show the final fit (thick line) together with the theoretical spectrum before convolution with the instrumental line spread function (thin dot-dashed line). The O I line at 927.7 Å is not saturated, the line at 927.2 Å is barely saturated, while the one at 978.9 Å is saturated. The bottom panels show the same data with the theoretical profiles using an O I column density reduced and increased by a factor of 10 (i.e. log N(OI) = 15.6 and 17.6, respectively). Such column densities are clearly excluded. With log N(OI) = 15.6, the line at 927.2 Å would not be detectable, and the line at 978.9 Å would be much fainter than observed. With log N(OI) = 17.6, the line at 927.7 Å would be much deeper than observed.

gas. Therefore the fitting of the O I lines has been performed with great care. Many of the O I lines are blended either with Galactic H I lines (O I lines at rest-wavelengths λ_0 = 916.8 Å, 918.0 Å, 930.2 Å, and 937.8 Å) or with Galactic H_2 lines (lines at λ_0 = 921.9 Å, 929.5 Å, 936.6 Å, 971.7 Å, and 988.7 Å) or with Galactic N I (λ_0 = 950.9 Å), or with the I Zw 18 H I Lyman δ line (λ_0 = 948.7 Å). The O I line at λ_0 = 1039 Å is strongly saturated and contaminated by a terrestrial airglow line, it is thus of no use for the column density determination. Finally we end up with the detection of three useful O I lines (λ_0 = 924.95 Å, 925.44 Å and 976.45 Å, see Table 2). We find $\log(N_{\rm cm^{-2}}(\mathrm{O\,I})) = 16.6^{+0.8}_{-0.55}$ (2-σ uncertainties, Fig. 2).

As a check, we also derived the O I column density by using the line at 1302 Å observed with the *GHRS* spectrograph and the *LSA* aperture of the *HST* on April 22, 1992. Individual *GHRS* "FP-split" exposures have been aligned by cross-correlation and co-added. The profile fitting has been done simultaneously for the *HST* and *FUSE* O I lines (see Table 2). Here, only the O I lines have been used to constrain the absorbing cloud parameters like the intrinsic line width b which is taken as a free parameter. We found $\log(N_{\rm cm^{-2}}(\mathrm{O\,I})) = 16.7^{+0.6}_{-0.7}$, which is consistent with the value derived from *FUSE* data alone (Table 1). However, to be conservative, as the λ_0 = 1302 Å line is strongly saturated and the *GHRS* aperture is very different from the *FUSE* aperture, we will adopt the value obtained with *FUSE* alone for further discussion.

Table 2. Oscillator strengths of a sample of useful N I and O I lines.

	λ_0 (Å)	$\lambda_{\rm obs}$ (Å)	f	Comment
N I	953.42	955.8	1.32×10^{-2}	not detected
N I	953.65	956.0	2.50×10^{-2}	"
N I	953.92	956.3	3.48×10^{-2}	faint detection
N I	954.10	956.5	0.68×10^{-2}	not detected
N I	963.99	966.4	1.48×10^{-2}	not detected
N I	964.63	967.0	0.94×10^{-2}	"
N I	965.04	967.4	0.40×10^{-2}	"
N I	1134.17	1137.0	1.52×10^{-2}	not detected
N I	1134.41	1137.2	2.97×10^{-2}	detected, not saturated
N I	1134.98	1137.8	4.35×10^{-2}	"
O I	924.95	927.2	1.59×10^{-3}	detected, slightly saturated
O I	925.44	927.7	0.35×10^{-3}	not detected
O I	976.45	978.9	3.31×10^{-3}	detected, saturated
O I	1039.23	1041.8	9.20×10^{-3}	strongly saturated + airglow
O I	1302.17	1305.4	51.9×10^{-3}	strongly saturated (*HST* observations)

4.1.5. N I

Lines of the N I triplet at 1134 Å are easily detected (Fig. 3). It is clear from the plot that the equivalent widths of the lines nicely follow the oscillator strengths (Table 2), indicating that these lines are not saturated. The simultaneous fit of these lines and other multiplets (at $\lambda_0 \approx$ 953 Å and $\lambda_0 \approx$ 964 Å) gives an accurate estimate of the N I column density: N(N I) = (1.7 ± 0.6) × 10^{14} cm^{-2} (2-σ).

4.1.6. Ar I, Si II, and Fe II

Two Ar I lines are present in the *FUSE* wavelength range. The one at λ_0 = 1066 Å is barely detected, while the strongest one at λ_0 = 1048 Å (4-time larger oscillator strength), is clearly detected but blended with a Galactic H_2 (J = 1) line (see Fig. 1 in Vidal-Madjar et al. 2000). Fortunately this Galactic H_2 (J = 1) is also detected in many other Lyman and Werner bands. Thanks to the `Owens` code, from a simultaneous fit to the complete set of data including all the H_2

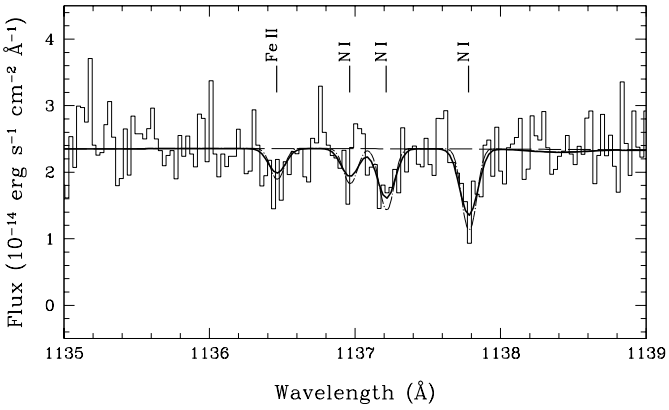

Fig. 3. Plot of the N I 1134 Å triplet in I Zw 18. The thick line is the fit to the data (histogram). The equivalent widths of the observed lines are proportional to their oscillator strengths, indicating these lines are not saturated. The mean column density of the gas is thus well constrained, even in the case of multiple lines of sight toward many bright stars (see Sect. 4.2).

and Ar I lines, we can estimate the argon column density to be $N(\mathrm{Ar\,I}) = 2.8^{+1.7}_{-1.2} \times 10^{13}$ cm^{-2}. These error bars include the uncertainties in the H_2 ($J = 1$) column density and in the instrumental profile. Consequently, they include also the uncertainties in the perturbation introduced by the blend with the H_2 line.

The Si II column density is derived from the strong line at $\lambda_0 = 989.9$ Å, and the line at $\lambda_0 = 1020.7$ Å which is also blended with a Galactic H_2 line (see Fig. 1 in Vidal-Madjar et al. 2000). We find $N(\mathrm{Si\,II}) = 6.3^{+4.9}_{-2.8} \times 10^{14}$ cm^{-2}.

The Fe II column density towards the UV bright stars of I Zw 18 is well constrained by a large set of Fe II lines that span a large range of oscillator strengths. From the simultaneous fit of all these lines we find $N(\mathrm{Fe\,II}) = 4.0^{+1.3}_{-0.8} \times 10^{14}$ cm^{-2}.

4.2. Multiple lines of sight

The analysis of absorption lines from galaxies raises a specific problem. The observed spectrum is the sum of the fluxes coming from thousands of hot stars through different absorbers with varying column densities and radial velocities.

For instance, the O I line at $\lambda_0 = 1039.23$ Å observed toward Mrk 59 is clearly larger than the line spread function and has a squared shape with a maximum absorption of about 25% (see Fig. 6 in Thuan et al. 2002). To fit that line, Thuan et al. (2002) added multiple profiles with radial velocities distributed over 100 km s^{-1} each having $b = 7$ km s^{-1}. However, such a particular velocity structure is not needed for I Zw 18. In effect, a careful inspection of the saturated O I line at $\lambda_{\rm obs} = 978.9$ Å shows that it goes almost to the zero level and that its width is not much larger than the width of the line before convolution with the instrumental profile (Fig. 2). All that indicates that the dispersion of the radial velocities of the individual clouds in the multiple lines of sight is not significantly larger than the intrinsic line width. The H I Lyman lines also shows that a special profile fitting procedure taking the multiple lines of sight into account is not needed for I Zw 18. Single Voigt profiles are sufficient to explain the lines structures. Thus the derived column densities for I Zw 18 are barely affected by the assumption of a single absorbing cloud in a single line of sight.

In addition, in the case of different lines of sight with similar column densities and intrinsic line widths but different radial velocities, the absorption profiles are well reproduced with single profiles convolved with a larger line spread function. All the lines observed towards I Zw 18, coming from I Zw 18, the Milky Way or the high velocity cloud at -160 km s^{-1}, can be fitted with the same instrumental line spread function. This reinforces the belief that the dispersion of the physical properties of the individual clouds in the different lines of sight toward I Zw 18 is limited.

Finally, for unsaturated lines like those of N I (Fig. 3), column densities obtained from a single Voigt profile are not affected by the complexity of the line of sight. For saturated lines like those of O I, a single Voigt profile can underestimate the saturation and thus column densities (see Thuan et al. 2002). However, in the case of O I, a larger column density would result in an O/H ratio larger in the H I gas than in the H II regions; this seems unlikely (see Sect. 5).

5. Discussion

5.1. The O/H ratio and the metallicity of the H I gas in I Zw 18

A main issue which can be addressed by the present observation is the comparison of the O/H ratio between the H I and the H II regions. We find $\log(\mathrm{O\,I/H\,I}) = -4.7^{+0.8}_{-0.6}$ (2-σ), in agreement with the O/H ratio measured in the H II region: $\log(\mathrm{O/H})_{\rm HII} = -4.83 \pm 0.03$ (Izotov et al. 1999). If the H I gas is more metal-deficient than the H II regions, the difference is at most 0.5 dex (at 2 σ).

From the analysis of the same *FUSE* data, Aloisi et al. (2003a, 2003b) found a significantly different value of the O I/H I ratio: $\log(\mathrm{O\,I/H\,I}) = -5.4 \pm 0.3$. if true, this would indicate that the H I gas is more metal-deficient than the H II regions. However their O I column density ($\log(N_{\rm cm^{-2}}(\mathrm{O\,I})) = 15.98 \pm 0.26$) is slightly below our 2-sigma limit. While this discrepancy is to be clarified, a likely source of a systematic error could be their use of the very saturated O I line at $\lambda_0 = 1039.23$ Å, which is contaminated by a terrestrial airglow.

Interestingly enough, O I/H I ratios similar to ours are found in two other blue compact dwarf galaxies: Mrk 59 ($\log(\mathrm{O\,I/H\,I}) = -5.0 \pm 0.3$ while $\log(\mathrm{O/H})_{\rm HII} = -4.011 \pm 0.003$, Thuan et al. 2002), and SBS 0035-052 ($\log(\mathrm{O\,I/H\,I}) = -5.0 \pm 1.1$ with $\log(\mathrm{O/H})_{\rm HII} = -4.70$). This may suggest that the metallicity of the surrounding neutral envelope of these blue galaxies is not related to the metallicity of the H II regions, which could have been self-enriched in metals by current or previous star formation bursts. However this may be coincidental; the error bars are large and Mrk 59 is up to now the only case for which a significant difference between the H I and H II regions has been found.

5.2. N/O ratio

The measured N I column density gives $\log(\mathrm{N\,I/O\,I}) = -2.4^{+0.6}_{-0.8}$ (2-σ), which is not consistent with a N/O ratio of about −1.5 expected at low metallicity for primary nitrogen. Even if some N I is ionized into N II, Jenkins et al. (2000) showed that the efficiency of photoionization arising from hot stars is at most 0.15 dex. Furthermore, nitrogen is only slightly depleted onto dust grains.

A possible explanation would be the ionization of N I by 40−80 eV photons arising from the recombinaison of He II, as suggested by Jenkins et al. (2000) in the case of the local interstellar medium. A similar nitrogen deficiency is also observed in about 40% of damped Lyman α systems which have apparently not yet reached the full primary nitrogen enrichment (Pettini et al. 2002). A possible explanation would be that the time delay for release of primary nitrogen is longer when metal abundances are lower (see Pettini et al. 2002 and references therein). Determination of N I and N II column densities in other blue compact dwarf galaxies is certainly needed to solve this puzzling low nitrogen content.

5.3. Ar/O ratio

Oxygen, silicon, and argon are α-chain elements produced by the same massive stars. As a consequence the Ar/O ratio is found almost constant in H II regions of blue compact dwarf galaxies (Thuan et al. 1995) or low surface-brightness dwarf galaxies (Van Zee et al. 1997) and close to the solar value: $\log(\mathrm{Ar\,I/O\,I}) \approx -2.3$.

In the neutral gas of I Zw 18 we measured $\log(\mathrm{Ar\,I/O\,I}) = -3.15^{+0.6}_{-0.85}$, a priori lower than expected. Although the *statistical* uncertainty in the Ar/O ratio is dominated by the much larger errors on the oxygen column density, Levshakov et al. (2001) raised the possibility of *systematic* errors on argon due to the complexity of the lines of sight. They showed that the column densities of argon, silicon, and iron can be significantly underestimated with the assumption of a single Voigt profile. Assuming a priori that the argon abundance is the same in the H I and the H II regions, they found a larger argon column density due to the saturation the argon line at λ_0 = 1048 Å. However, these authors fitted only the line at λ_0 = 1048 Å; they did not fit the fainter line at λ_0 = 1066 Å. Even with the column density given by Levshakov et al. (2001) ($\log(N_{\mathrm{cm}^{-2}}(\mathrm{Ar\,I})) \sim 14.46$), and a simple line of sight, this line at λ_0 = 1066 Å is not saturated. It appears difficult to have a complex line of sight which leads to an underestimation by a factor of 10 in the equivalent width of this line, and simultaneously an O I line which goes to almost zero at λ_{obs} = 978.9 Å (see Fig. 2 and Sect. 4.2).

A more likely explanation of the apparently low Ar I/O I ratio is a significant fraction of Ar I ionized into Ar II. This ionization is supposed to be responsible for the low Ar I/H I ratio measured in the local interstellar medium, lower than the cosmic value of Ar/H (Jenkins et al. 2000). In general, the argon is more strongly ionized than hydrogen because the cross section for the photoionization of Ar I is very high. Jenkins et al. (2000) showed that the deficiency in Ar I caused by the photoionization can be down to ∼−0.4 dex for a shielding against the ionization photons of $N(\mathrm{H\,I}) \sim 10^{18}$ cm^{-2}.

Nonetheless, the large error bars on the oxygen column density could itself partially solve the issue of the apparent low Ar I/O I ratio.

As a summary, the Ar I/O I ratio provides two different clues. First, a hint towards a significant ionization of argon as observed in the local interstellar medium. Second, a hint of the favored oxygen column density within the measured 2-σ interval. For example a value around $\log(N_{\mathrm{cm}^{-2}}(\mathrm{O\,I})) \sim 16.3$ would give $\log(\mathrm{Ar\,I/O\,I}) \sim -2.8$ and $\log(\mathrm{Si\,II/O\,I}) \sim -1.5$. The Ar I/O I ratio would be thus consistent with the standard value, with a partial ionization. The Si/O ratio would be the same as the value measured in the I Zw 18 H II region (Izotov et al. 1999).

6. Conclusion

We have measured column densities of H I, N I, O I, Ar I, Si II, Fe II in the neutral gas of I Zw 18. We obtain the following results:

1. The measured O I/H I ratio is consistent with the O/H ratio as observed in the H II regions. We find $\log(\mathrm{O\,I/H\,I}) = -4.7^{+0.85}_{-0.6}$ (2-σ) which is also consistent with the O/H ratios ∼−5 measured with *FUSE* in the H I regions of other blue compact galaxies. If the oxygen is depleted in the H I region compared to the H II regions, the depletion is at most 0.5 dex in I Zw 18.
2. The measured N I/O I ratio is $\log(\mathrm{N\,I/O\,I}) = -2.4^{+0.6}_{-0.8}$ (2-σ). This is lower than the value of −1.5 expected for the N/O ratio with primary nitrogen. The determination of the N II column density is needed to discriminate between an ionization of N I or a possible nitrogen deficiency.
3. The neutral argon is also apparently underabundant. A significant ionization into Ar II appears likely. The small error bars in the determination of Ar I and Si II column densities favor the lower values of the large error bars in the O I column density, around $\log(N_{\mathrm{cm}^{-2}}(\mathrm{O\,I})) \sim 16.3$.

Acknowledgements. This work has been done using the profile fitting procedure developed by M. Lemoine and the *FUSE* French Team. The data were obtained for the Guaranteed Time Team by the NASA-CNES-CSA *FUSE* mission operated by the Johns Hopkins University. Financial support for French participants has been provided by CNES. We warmly thank G. Östlin, J. Lequeux and J. M. Mas-Hesse for fruitful discussions. We thank the anonymous referee for helpful remarks.

References

Aloisi, A., Savaglio, S., Heckman, T. M., et al. 2003a, BAAS, 35
Aloisi, A., Savaglio, S., Heckman, T. M., et al. 2003b, ApJ, in press
Brown, T. M., Heap, S. R., Hubeny, I., Lanz, T., & Lindler, D. 2002, ApJ, 579, L75
Hébrard, G., Lemoine, M., Vidal-Madjar, A., et al. 2002, ApJS, 140, 103
Izotov, Y. I., & Thuan, T. X. 1999, ApJ, 511, 639
Jenkins, E. B., Oegerle, W. R., Gry, C., et al. 2000, ApJ, 538, L81
Kunth, D., & Sargent, W. L. W. 1986, ApJ, 300, 496

Kunth, D., Lequeux, J., Sargent, W. L. W., & Viallefond, F. 1994, A&A, 282, 709
Kunth, D., Matteucci, F., & Marconi, G. 1995, A&A, 297, 634
Lebouteiller, V., Kunth, D., et al. 2003, A&A, in preparation
Lecavelier des Etangs, A., Thuan, T. X., & Izotov, Y. I. 2002, FUSE Science and Data Workshop, III, 59
Lemoine, M., Vidal-Madjar, A., Hébrard, G., et al. 2002, ApJS, 140, 67
Lequeux, J., & Viallefond, F. 1980, A&A, 91, 269
Levshakov, S. A., Kegel, W. H., & Agafonova, I. I. 2001, A&A, 373, 836
Moos, H. W., Cash, W. C., Cowie, L. L., et al. 2000, ApJ, 538, L1
Pettini, M., Ellison, S. L., Bergeron, J., & Petitjean, P. 2002, A&A, 391, 21
Pettini, M., & Lipman, K. 1995, A&A, 297, L63
Sahnow, D. J., Moos, H. W., Ake, T. B., et al. 2000, ApJ, 538, L7
Savage, B. D., Sembach, K. R., Wakker, B. P., et al. 2003, ApJS, 146, 125
Sembach, K. R., Wakker, B. P., Savage, B. D., et al. 2003, ApJS, 146, 165
Thuan, T. X., Izotov, Y. I., & Lipovetsky, V. A. 1995, ApJ, 445, 108
Thuan, T. X., Izotov, Y. I., & Lipovetsky, V. A. 1997, ApJ, 477, 661
Thuan, T. X., Lecavelier des Etangs, A., & Izotov, Y. I. 2002, ApJ, 565, 941
Thuan, T. X., Lecavelier des Etangs, A., & Izotov, Y. I. 2003, ApJ, in preparation
van Zee, L., Haynes, M. P., & Salzer, J. J. 1997, AJ, 114, 2497
van Zee, L., Westpfahl, D., Haynes, M. P., & Salzer, J. J. 1998, AJ, 115, 1000
Viallefond, F., Lequeux, J., & Comte, G. 1987, in Starbursts and galaxy evolution, ed. T. X. Thuan, T. Montmerle, & J. Tran Thanh Van (Éditions Frontières), 139
Vidal-Madjar, A., Kunth, D., Lecavelier des Etangs, A., et al. 2000, ApJ, 538, L77
Wakker, B. P., Savage, B. D., Sembach, K. R., et al. 2003, ApJS, 146, 1